Analyses of effective viscosity of suspensions with deformable polydispersed spheres

Article *in* Journal of Physics D Applied Physics · March 2009

DOI: 10.1088/0022-3727/42/7/075503

CITATIONS
10

READS
278

2 authors:

Chun-Hway Hsueh
National Taiwan University
306 PUBLICATIONS **8,249** CITATIONS
SEE PROFILE

Wen-Cheng Wei
National Taiwan University
157 PUBLICATIONS **2,485** CITATIONS
SEE PROFILE

IOP PUBLISHING JOURNAL OF PHYSICS D: APPLIED PHYSICS

J. Phys. D: Appl. Phys. **42** (2009) 075503 (7pp) doi:10.1088/0022-3727/42/7/075503

Analyses of effective viscosity of suspensions with deformable polydispersed spheres

C H Hsueh[1,2,3,4] **and W C J Wei**[1]

[1] Department of Materials Science and Engineering, National Taiwan University, Taipei 106, Taiwan
[2] Department of Physics and Astronomy, University of Tennessee, Knoxville, TN 37996, USA

E-mail: hsuehc@ornl.gov

Received 22 January 2009, in final form 21 February 2009
Published 20 March 2009
Online at stacks.iop.org/JPhysD/42/075503

Abstract

A simple expression is derived for the effective shear viscosity of suspensions with deformable polydispersed spheres in this study. The analyses commence with the modified Eshelby model to derive the elastic stress–strain relation for an elastic composite containing spherical inclusions. Then, using the elastic–viscous analogy, the effective shear viscosity is obtained for suspensions with small volume fractions of deformable mono-sized spheres. Finally, using Bruggeman's differential model, the formula for the effective shear viscosity of suspensions with concentrated deformable polydispersed spheres is obtained. The present formulae are compared with some of the existing solutions and experimental measurements, and good agreement is obtained.

1. Introduction

Concentrated suspensions have attracted great interest because of their applications in processing of ceramics, food, beverage, pharmacy, paints, magmas and cosmetic industries, etc [1–9]. Rheology studies of suspensions provide insight into the interparticle interactions, and viscosity is the most measured rheological property. The pioneering work on the effective viscosity of suspensions was performed by Einstein in which the motion of a single rigid sphere in a fluid was considered and the effective (shear) viscosity of suspensions of spheres, η^*, was derived as a function of the viscosity of the pure liquid, η_o, as well as the volume fraction of rigid spheres, ϕ, such that [10]

$$\eta^* = \eta_o(1 + 2.5\phi). \tag{1}$$

Einstein's equation is valid for a very dilute dispersion of rigid spheres, and its applicability has been extended to higher volume fractions of rigid spheres by including interactions between spheres in analyses [11–19]. The problem is generally analysed by using the Navier–Stokes equation to describe the velocity field of the viscous fluid, which is perturbed by the presence of spheres. The spheres are generally considered to be rigid and mono-sized, and both long-range hydrodynamic interactions and short-range interparticle forces are considered. The dynamics of the fluid and spheres are coupled by the boundary condition that the fluid and sphere velocities match at the sphere's surface (i.e. the no slip boundary condition). It has been concluded that Einstein's equation can be extended to account for effects of sphere interactions by adding higher-order volume-fraction terms, such that

$$\eta^* = \eta_o(1 + 2.5\phi + c\phi^2 + \cdots). \tag{2}$$

However, there is no general agreement on the principles by which coefficients for the order of the second and higher terms are to be calculated. This is because of the complexity in the mathematical treatment of the integral equations that describe interactions between spheres. Also, the calculated results depend on whether two-sphere interactions or many-sphere interactions are considered, which spatial distribution function is used for the spheres and how the integral is calculated in powers of ϕ. As a result, different values for the ϕ^2 coefficient, c, have been obtained [11–19].

For viscous spheres with a finite viscosity, η_s, the problem is complicated by not only η_s but also the capillary number, Ca, which represents the relative effect of the viscous force

[3] Author to whom any correspondence should be addressed.

[4] Materials Science and Technology Division, Oak Ridge National Laboratory, Oak Ridge, TN 37831, USA (on leave).

and the surface tension, γ, of spheres [6] and is defined by $\mathrm{Ca} = \eta_o v/\gamma$, where v is a characteristic velocity. For small Ca, deformation of spheres is controlled by surface tension and viscous spheres remain spherical in the suspension. For large Ca, viscous spheres are deformed by the hydrodynamic stress in the suspension. The classical work by Taylor [20] considered that the emulsifier film around spheres would not prevent stress transfer from the fluid to the dispersed viscous spheres and that there was no slippage at the sphere–fluid interface. By extending Einstein's analysis, Taylor obtained [20]

$$\eta^* = \eta_o \left[1 + 2.5\phi \left(\frac{\eta_s + 0.4\eta_o}{\eta_s + \eta_o}\right)\right]. \tag{3}$$

Like Einstein's equation, equation (3) is valid for dilute suspensions. When the viscous spheres become rigid (i.e. $\eta_s \to \infty$), equation (3) is reduced to Einstein's equation, equation (1). However, it should be noted that not all the essential continuity conditions at the sphere–fluid interface are satisfied in Tayor's model. Specifically, while continuities of velocity and tangential stresses are satisfied, continuity of normal stress is not, and the deformation of spheres is not considered. In this case, Taylor's solution is pertinent to the system with small values of Ca. It should also be noted that if a viscoelastic membrane forms on the sphere surface, the membrane will retard the transmittance of tangential stress from the fluid to spheres and therefore hinders the flow within spheres. In this case, the viscous spheres act like hard spheres.

To extend the solution for dilute suspensions to that for concentrated suspensions, a simple differential model has been developed by Bruggeman [21]. The basic idea is to construct concentrated suspensions from a fluid through a series of incremental additions of spheres until its final volume fraction is reached. At each stage of the process, the relevant solution of a dilute suspension problem is used to construct the effective properties of the suspension, which is then used as the base viscosity for the next incremental step. Because the base suspension is treated as a homogeneous effective medium when an infinitesimal number of spheres are added, the added spheres at each step should be larger than the spheres added in the previous step. Hence, the differential model is pertinent to the case of polydispersed suspensions. Roscoe [22] applied the differential model to Einstein's equation to obtain η^* for suspensions of polydispersed hard spheres. Combining Taylor's equation and Bruggeman's differential model, Phan-Thien and Pham [23] derived the effective viscosity for suspensions with non-deformable polydispersed spheres.

The purpose of this study is to derive the effective viscosity for polydispersed concentrated suspensions with deformable viscous spheres (i.e. large values of Ca). To achieve this, the modified Eshelby model [24, 25] for effective Young's modulus of an elastic composite containing spherical inclusions [26], the elastic–viscous analogy for converting elastic to viscous solutions [27, 28] and Bruggeman's differential model [21] are used. Then the present formulae are compared with (i) the predictions obtained from other models [23, 29, 30] and (ii) the experimental measurements for the effective viscosity of concentrated suspensions with deformable polydispersed bubbles [31, 32].

2. Analyses

To derive the effective viscosity for polydispersed concentrated suspensions with deformable viscous spheres (i.e. large capillary numbers), the present analyses consist of three analytical procedures: (i) the modified Eshelby model is used to derive the elastic stress–strain relation for an elastic composite containing spherical inclusions. (ii) The elastic–viscous analogy is adopted to obtain the effective shear viscosity for suspensions with small volume fractions of deformable mono-sized spheres. (iii) Bruggeman's differential model is applied to derive the formula for the effective shear viscosity of suspensions with concentrated deformable polydispersed spheres.

2.1. Modified Eshelby model

It has been noted that the solution of viscous deformation of suspensions can be obtained from the solution of elastic deformation of composites using the elastic–viscous analogy [27, 28]. A model for analysing the elastic stress field of an infinite matrix containing an ellipsoidal inclusion was first developed by Eshelby [24]. Considering the average stress imposed on an inclusion due to the presence of other inclusions, the Eshelby model was modified to include the effect of a finite volume fraction of inclusions by Mori and Tanaka [25]. Using the modified Eshelby model, the elastic stress transfer between the matrix and aligned ellipsoidal inclusions was derived by Hsueh [26]. The formulations of Hsueh's solutions are formidable because of the complex Eshelby tensor involved; however, the tensor components are greatly simplified when inclusions are spherical and Poisson's ratio is 0.5. It can be derived from Hsueh's results that the uniaxial stress–strain (i.e. σ–ε) relation for elastic composites containing spherical inclusions is

$$\varepsilon = \left[\frac{2G_s + 3G_o - 2\phi(G_s - G_o)}{2G_s + 3G_o + 3\phi(G_s - G_o)}\right]\frac{\sigma}{E_o} \quad (\text{for } \nu_s = \nu_o = 0.5), \tag{4}$$

where E, ν and G are Young's modulus, Poisson's ratio and shear modulus, respectively, and the subscripts, s and o, denote spherical inclusion and matrix, respectively.

It should be noted that the details of the spatial distribution of inclusions are not considered in the modified Eshelby model, and the mean field is considered in modelling. Also, in the absence of inclusions, the deformation throughout the system is uniform and is described by $\varepsilon = \sigma/E_o$ for uniaxial loading. The deformation of inclusions is reflected by the uniaxial stress–strain relation shown in equation (4). Specifically, spherical inclusions become ellipsoids when the composite is subjected to uniaxial loading which is described by the constrained strain component in inclusions in [24–26].

2.2. Elastic–viscous analogy

In using the elastic–viscous analogy, the procedures of Laplace transform and inverse Laplace transform are required to obtain viscous solutions from elastic solutions [27, 28, 33]. However, it has been derived that these procedures are equivalent to

making the following replacements: $\varepsilon \rightarrow \dot{\varepsilon}$, $\nu \rightarrow 0.5$, $E \rightarrow 3\eta$ and $G \rightarrow \eta$, where $\dot{\varepsilon}$ is the uniaxial strain rate of the corresponding viscous composite. Hence, the shear viscosity, η^*, of viscous composites is

$$\eta^* = \frac{\sigma}{3\dot{\varepsilon}} = \eta_o \left[\frac{2\eta_s + 3\eta_o + 3\phi(\eta_s - \eta_o)}{2\eta_s + 3\eta_o - 2\phi(\eta_s - \eta_o)} \right]. \quad (5)$$

Equation (5) is identical to Bedeaux's solution [34] for the effective shear viscosity of the two-phase flow when ϕ is small. It should be noted that the details of the velocity gradients due to the variation of the viscosity in space and time were not considered in Bedeaux's analysis. Instead, the average of velocity fields over regions sufficiently large compared with the structure was considered to derive the effective viscosity of the suspension [34]. Equation (5) is also identical to Hashin and Shtrikman's lower-bound solution for the effective shear modulus of incompressible composites based on a composite-sphere model [30] while Hashin and Shtrikman's upper-bound solution is given by [30]

$$\eta^* = \eta_s \left[\frac{5\eta_o - 3\phi(\eta_o - \eta_s)}{5\eta_s + 2\phi(\eta_o - \eta_s)} \right]. \quad (6)$$

However, it should be noted that the above bound solutions, equations (5) and (6), are valid when $\eta_s > \eta_o$. If $\eta_s < \eta_o$, the two equations should be exchanged; that is, equations (5) and (6) become the upper- and the lower-bound solutions, respectively.

Because all the essential continuity conditions at the inclusion–matrix interface are satisfied in the Eshelby model, the spheres are considered as deformable in analyses. Hence, equation (5) is pertinent to the system of suspensions with large values of Ca. However, because only the average stress imposed on an inclusion due to the presence of other inclusions is considered in the modified Eshelby model, η^* obtained from equation (5) through the analogy contains only long-range interactions. With the lack of short-range interparticle forces, equation (5) would not be accurate in describing the effective viscosity of suspensions with high volume fractions of spheres. Nevertheless, when ϕ is sufficiently small, the neglect of short-range interparticle forces can be justified. Hence, when $\phi \rightarrow 0$, equation (6) can be simplified to

$$\eta^* = \eta_o \left[1 + 2.5\phi \left(\frac{\eta_s - \eta_o}{\eta_s + 1.5\eta_o} \right) \right] \qquad (\text{for } \phi \rightarrow 0). \quad (7)$$

Equation (7) describes the effective viscosity of the suspension, η^*, when a small volume fraction ϕ of deformable spheres with viscosity η_s is added to a fluid with viscosity η_o.

2.3. Bruggeman's differential model

The differential model constructs the suspension by adding an infinitesimal volume fraction of spheres at each step. At any intermediate step, the volume fraction of spheres in the suspension is defined as ϕ and the effective viscosity of suspension is defined as η^*. When an infinitesimal volume fraction $\Delta\phi$ of spheres is added to this suspension, the newly added spheres have a volume fraction $\Delta\phi/(1 + \Delta\phi)$ in the new suspension and the effective viscosity of the suspension changes from η^* to $\eta^*+\mathrm{d}\eta^*$. Using equation (7), the differential model yields

$$\eta^* + \mathrm{d}\eta^* = \eta^* \left[1 + 2.5 \left(\frac{\Delta\phi}{1 + \Delta\phi} \right) \left(\frac{\eta_s - \eta^*}{\eta_s + 1.5\eta^*} \right) \right]. \quad (8)$$

At this step, the total volume fraction of spheres increases from ϕ to $\phi + \mathrm{d}\phi$, such that

$$\phi + \mathrm{d}\phi = \frac{\phi + \Delta\phi}{1 + \Delta\phi}. \quad (9)$$

Based on equation (9), $\mathrm{d}\phi$ is related to $\Delta\phi$ by

$$\mathrm{d}\phi = \frac{(1 - \phi)\,\Delta\phi}{1 + \Delta\phi}. \quad (10)$$

Combination of equations (8) and (10) yields

$$\frac{(\eta_s + 1.5\eta^*)\,\mathrm{d}\eta^*}{2.5(\eta_s - \eta^*)\eta^*} = \frac{\mathrm{d}\phi}{1 - \phi}. \quad (11)$$

Integration of equation (11) with the initial condition, $\eta^* = \eta_o$ at $\phi = 0$, yields

$$\phi = 1 - \left(\frac{\eta_o}{\eta^*} \right)^{2/5} \frac{\eta_s - \eta^*}{\eta_s - \eta_o}. \quad (12)$$

Equation (12) is the expression for the effective shear viscosity of suspensions with deformable polydispersed spheres. However, it should be noted that the details of the spatial and the size distributions of spheres are not considered in deriving equation (12).

When $\eta_s \rightarrow \infty$, equation (12) becomes

$$\eta^* = \eta_o(1 - \phi)^{-2.5} \qquad (\text{for } \eta_s \rightarrow \infty). \quad (13)$$

Equation (13) is identical to Roscoe's equation [22] for the viscosity of suspensions of polydispersed rigid spheres. For small volume fractions of polydispersed spheres (i.e. $\phi \rightarrow 0$), equation (13) is further reduced to Einstein's equation, equation (1). When spheres become bubbles (i.e. $\eta_s = 0$), equation (12) becomes

$$\eta^* = \eta_o(1 - \phi)^{5/3} \qquad (\text{for } \eta_s = 0). \quad (14)$$

In this case, η^* decreases with increasing volume fraction of bubbles.

2.4. Consideration of maximum packing volume fraction of spheres

It has been noted that the differential model imposes no restriction on the volume fraction of dispersed spheres, ϕ, and the value of ϕ can reach unity. This is physically unrealistic. With the volume fraction ϕ of spheres in the fluid, the free volume in the fluid available is less than $1–\phi$ when new spheres are added to the fluid because a significant portion of the fluid is immobilized in the volume between existing spheres. To account for this, it has been suggested that the effective volume occupied by spheres is ϕ/ϕ_c instead of ϕ where ϕ_c

is an adjustable parameter related to the volume fraction at which spheres become closely packed. The typical value of ϕ_c is between 0.6 and 0.7 [35]. Hence, when an infinitesimal volume fraction $\Delta\phi$ of spheres is added to the suspension, the total effective volume fraction of spheres increases from ϕ/ϕ_c to $\phi/\phi_c + d\phi$, such that

$$\phi/\phi_c + d\phi = \frac{\phi/\phi_c + \Delta\phi}{1 + \Delta\phi}. \tag{15}$$

Using equation (15), $d\phi$ is related to $\Delta\phi$ by

$$d\phi = \frac{(1 - \phi/\phi_c)\Delta\phi}{1 + \Delta\phi}. \tag{16}$$

Replacing equation (10) by equation (16) in the differential model, it can be derived that equation (12) becomes

$$\phi = \phi_c \left[1 - \left(\frac{\eta_o}{\eta^*}\right)^{\frac{2}{5\phi_c}} \left(\frac{\eta_s - \eta^*}{\eta_s - \eta_o}\right)^{\frac{1}{\phi_c}} \right]. \tag{17}$$

When $\eta_s \to \infty$, equation (17) is reduced to the well-known Dougherty and Krieger equation [35] for suspensions with rigid spheres, such that

$$\eta^* = \eta_o \left(1 - \frac{\phi}{\phi_c}\right)^{-2.5\phi_c}. \tag{18}$$

3. Comparison

First, Phan-Thien and Pham's solution for the effective viscosity for suspensions with non-deformable polydispersed spheres and the solution obtained by Christensen, who used a micro-mechanics model and a generalized self-consistent method to derive the effective viscosity for polydispersed concentrated suspensions, are summarized. Then a comparison is made between the present and existing analytical results and experimental measurements.

3.1. Phan-Thien and Pham's solution

Phan-Thien and Pham [23] derived the effective viscosity for polydispersed concentrated suspensions by combining Taylor's equation [20] and Bruggeman's differential model [21], and the solution is

$$\phi = 1 - \left(\frac{\eta_o}{\eta^*}\right)^{2/5} \left(\frac{2.5\eta_s + \eta_o}{2.5\eta_s + \eta^*}\right)^{3/5}. \tag{19}$$

Phan-Thien and Pham's solution, equation (19), is pertinent to emulsions with small capillary numbers such that spherical droplets remain spherical in the suspension. The difference between the present formula and Phan-Thien and Pham's solution can be observed by comparing equation (12) with equation (19). When $\eta_s \to \infty$, both equations (12) and (19) can be reduced to equation (13) for the viscosity of suspensions of polydispersed rigid spheres. However, when spheres become bubbles (i.e. $\eta_s = 0$), equation (19) becomes

$$\eta^* = \frac{\eta_o}{1 - \phi} \qquad (\text{for } \eta_s = 0). \tag{20}$$

Hence, the viscosity of suspensions increases with the volume fraction of bubbles. This is because bubbles are considered to remain spherical and non-deformable in the suspension in Taylor's model.

3.2. Christensen's solution

Using a micro-mechanics model, Christensen [29] developed a generalized self-consistent method to derive the effective properties of polydispersed suspensions. Based on Christensen's solution for incompressible suspension (i.e. letting Poisson's ratio = 0.5), η^* satisfies a quadratic equation, such that

$$A\left(\frac{\eta^*}{\eta_o}\right)^2 + 2B\left(\frac{\eta^*}{\eta_o}\right) + C = 0, \tag{21}$$

where

$$A = 12\eta_1\left(\frac{\eta_s}{\eta_o} - 1\right)\phi^{10/3} - 2\left[63\eta_2\left(\frac{\eta_s}{\eta_o} - 1\right) + 2\eta_1\eta_3\right]\phi^{7/3} + 252\eta_2\left(\frac{\eta_s}{\eta_o} - 1\right)\phi^{5/3} - 150\eta_2\left(\frac{\eta_s}{\eta_o} - 1\right)\phi + 8\eta_2\eta_3,$$

$$B = 3\eta_1\left(\frac{\eta_s}{\eta_o} - 1\right)\phi^{10/3} + 2\left[63\eta_2\left(\frac{\eta_s}{\eta_o} - 1\right) + 2\eta_1\eta_3\right]\phi^{7/3} - 252\eta_2\left(\frac{\eta_s}{\eta_o} - 1\right)\phi^{5/3} + 93.75\eta_2\left(\frac{\eta_s}{\eta_o} - 1\right)\phi + 0.75\eta_2\eta_3,$$

$$C = -18\eta_1\left(\frac{\eta_s}{\eta_o} - 1\right)\phi^{10/3} - 2\left[63\eta_2\left(\frac{\eta_s}{\eta_o} - 1\right) + 2\eta_1\eta_3\right]\phi^{7/3} + 252\eta_2\left(\frac{\eta_s}{\eta_o} - 1\right)\phi^{5/3} - 168.75\eta_2\left(\frac{\eta_s}{\eta_o} - 1\right)\phi - 9.5\eta_2\eta_3$$

with

$$\eta_1 = 19\left(\frac{\eta_s}{\eta_o} - 1\right), \quad \eta_2 = 9.5\left(\frac{\eta_s}{\eta_o} - 1\right) + 17.5,$$

$$\text{and} \quad \eta_3 = 3\left(\frac{\eta_s}{\eta_o} - 1\right) + 7.5.$$

3.3. Comparison

The present analytical results are compared with the existing analytical results and experimental measurements. First, suspensions with deformable polydispersed viscous spheres are considered, and the results obtained from equation (12) are compared with the results from Hashin and Shtrikman's bound solutions, equations (5) and (6), and Christensen's solution, equation (21). Second, the difference between suspensions with deformable and non-deformable polydispersed viscous spheres is considered, and the results obtained from equation (12) are compared with those from Phan-Thien and Pham's equation, equation (19). Finally, suspensions with deformable polydispersed bubbles are considered, and the results obtained from equations (12) and (17) are compared with existing numerical results [36] and measurements [31, 32].

The normalized effective viscosities of suspensions, η^*/η_o, as functions of the volume fraction of deformable

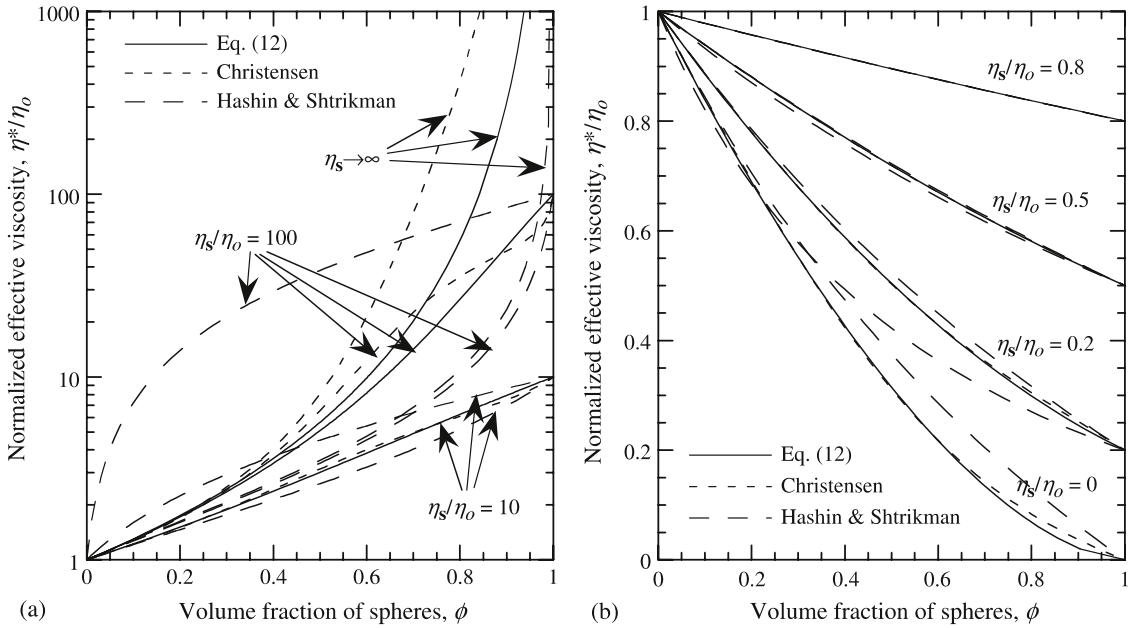

Figure 1. The normalized effective viscosity, η^*/η_o, of suspensions as a function of the volume fraction of deformable polydispersed spheres, ϕ, for the sphere-to-liquid viscosity ratio, η_s/η_o, being (a) 10, 100 and ∞ and (b) 0, 0.2, 0.5 and 0.8 showing the comparison among the present formula, equation (12), Hashin and Shtrikman's bound solutions, equations (5) and (6), and Christensen's solution, equation (21).

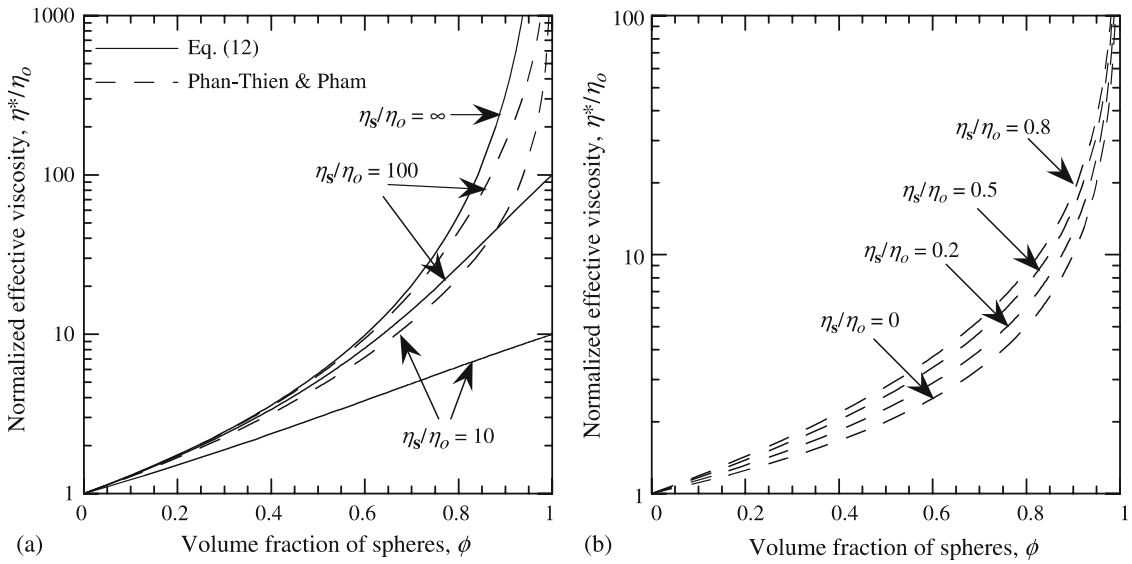

Figure 2. The normalized effective viscosity, η^*/η_o, of suspensions as a function of the volume fraction of polydispersed spheres, ϕ, for the sphere-to-liquid viscosity ratio, η_s/η_o, being (a) 10, 100 and ∞ showing the difference between deformable and non-deformable spheres and (b) 0, 0.2, 0.5 and 0.8 showing the results for non-deformable spheres to compare with figure 1(b).

polydispersed spheres, ϕ, are shown in figures 1(a) and (b), respectively, for the sphere-to-fluid viscosity ratio, η_s/η_o, being greater and lesser than unity. When $\eta_s/\eta_o > 1$, figure 1(a) shows that η^*/η_o increases with both ϕ and η_s/η_o. When $\eta_s/\eta_o < 1$, figure 1(b) shows that η^*/η_o increases with increasing η_s/η_o but decreases with increasing ϕ. The difference between Hashin and Shtrikman's upper- and lower-bound solutions increases when η_s/η_o deviates from unity. Specifically, the upper-bound solution shows that $\eta^* \to \infty$ when $\eta_s \to \infty$, and the lower-bound solution shows that $\eta^* = 0$ when $\eta_s = 0$. Hashin and Shtrikman's solutions for these two extreme cases are not shown in figures 1(a) and (b). However, both the present formula and Christensen's solution are always within Hashin and Shtrikman's bound solutions. Also, the present formula and Christensen's solution are in excellent agreement for $\eta_s/\eta_o \leqslant 10$, and the curves from these two solutions can hardly be distinguished in some cases in figure 1(b) for fixed η_s/η_o.

The normalized effective viscosity of suspensions, η^*/η_o, as a function of the volume fraction of polydispersed spheres, ϕ, is plotted in figure 2(a) for $\eta_s/\eta_o > 1$ to show the difference between deformable and non-deformable spheres, i.e. equations (12) and (19). The normalized effective viscosity of suspensions, η^*/η_o, as a function of the volume fraction

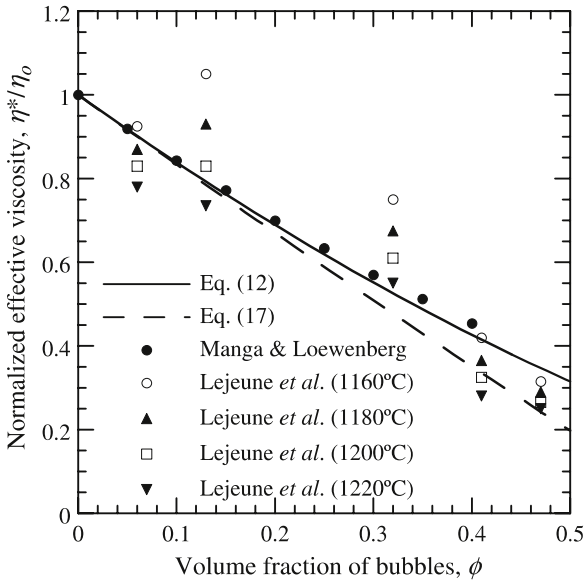

Figure 3. The normalized effective viscosity, η^*/η_o, of suspensions as a function of the volume fraction of deformable spherical bubbles, ϕ, showing the comparison among the present formulae, equations (12) and (17), Manga and Loewenberg's numerical simulations and Lejeune *et al*'s measurements.

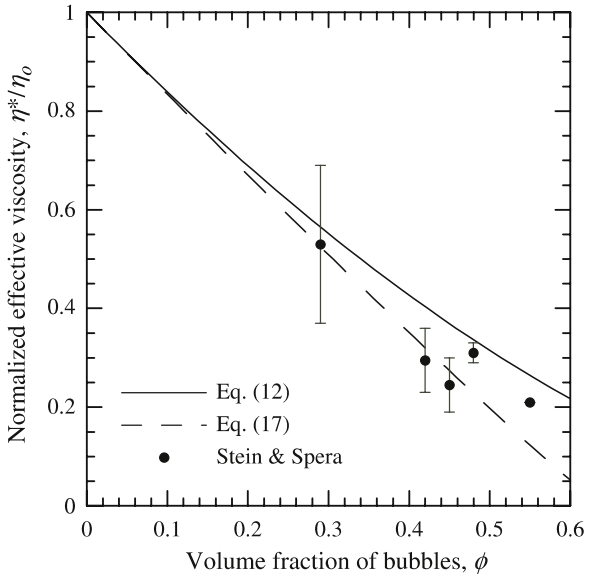

Figure 4. The normalized effective viscosity, η^*/η_o, of suspensions as a function of the volume fraction of deformable bubbles, ϕ, showing the comparison between the present formulae, equations (12) and (17), and Stein and Spera's measurements. (This figure is in colour only in the electronic version)

of non-deformable polydispersed spheres, ϕ, is shown in figure 2(*b*) for $\eta_s/\eta_o < 1$ while the corresponding solutions for deformable spheres can be found in figure 1(*b*). Equations (12) and (19) become identical only when the spheres are rigid. Otherwise, compared with equation (12), equation (19) always predicts a higher value of η^*. Specifically, figure 2(*b*) shows that η^*/η_o is always greater than unity even when η_s/η_o is less than unity, and both figures 2(*a*) and (*b*) show that $\eta^* \to \infty$ when $\phi \to 1$ regardless of the value of η_s when the spheres are non-deformable.

Bubbles formed by exsolution of volatiles play a major role in magma ascent and volcanic eruptions, and rheology of bubble-bearing magmas is of interest. It has been concluded that magmas have large capillary numbers because of their high viscosity and bubbles are deformable in magmas [6]. Using the boundary integral numerical technique, Manga and Loewenberg [36] performed numerical simulations to calculate the viscosity of a suspension of deformable spherical bubbles within a Newtonian fluid, and the calculated results are shown in figure 3. It should be noted that mono-sized bubbles were considered in the simulation, and the upper value on ϕ of 0.4 shown in figure 3 is governed by the maximum number of bubbles that can be randomly positioned inside the unit cell in simulations. Lejeune *et al* [31] measured the viscosity of the calcium alumiosilicate melt containing deformable polydispersed bubbles at high temperatures, and the results are also shown in figure 3. Using $\phi_c = 0.64$, η^* is predicted from equation (17). Compared with equation (17), equation (12) has a better agreement with Manga and Loewenberg's numerical results. However, no conclusion can be drawn because polydispersed spheres are considered in deriving equations (12) and (17), while mono-sized bubbles are considered in simulations. Although the suspensions have polydispersed bubbles in measurements, the spread of data makes it difficult to judge whether equation (12) or equation (17) gives a better prediction.

Stein and Spera [32] measured the shear viscosity of rhyolite-bubble emulsions at magmatic temperatures. The bubble sizes have a log-normal distribution, and the experiments were carried out at high capillary numbers with $30 < \mathrm{Ca} < 925$. The measured relative viscosity as a function of the volume fraction of bubbles is shown in figure 4. It was claimed that the measured viscosities were not sensitive to the temperature for the temperature range 925–1125 °C in the experiment. The variation of the measured viscosities at a fixed porosity is due to inter-sample variability associated with (1) the heterogeneous distribution of bubbles, (2) the presence of a range of bubble sizes and (3) experimental uncertainty [32]. Again, the spread of data in figure 4 makes it difficult to judge whether equation (12) or equation (17) gives a better prediction.

4. Conclusions

Since Einstein derived the effective viscosity of suspensions with dilute dispersion of rigid spheres, significant efforts have been made to extend the solution to the case of higher volume fractions of spheres. The spheres can be mono-sized or polydispersed, and they can also be rigid or viscous. When the spheres are viscous, the solutions also depend on the relative effect of the viscous force and the surface tension of spheres, i.e. the capillary number. For small capillary numbers, deformation of spheres is controlled by surface tension and viscous spheres remain spherical in the suspension. For large capillary numbers, viscous spheres are deformed by the hydrodynamic stress in the suspension. Using the modified Eshelby model, the elastic–viscous analogy and

Bruggeman's differential model, formulae for the effective shear viscosity of suspensions with deformable polydispersed spheres are derived in this study. Compared with the existing solutions, our formula, equation (12), is (i) within Hashin and Shtrikman's bound solutions, (ii) much more concise than Christensen's solution, equation (21), and (iii) in excellent agreement with Christensen's solution when the sphere-to-liquid viscosity ratio is less than 10. Our formula is also in good agreement with Manga and Loewenberg's simulated results for suspensions of deformable spherical bubbles within a Newtonian fluid. Compared with existing experimental results, good agreement is obtained with (i) Lejeune *et al*'s viscosity measurements of calcium alumiosilicate melt containing deformable polydispersed bubbles at high temperatures and (ii) Stein and Spera's viscosity measurements of rhyolite-bubble emulsions at magmatic temperatures.

Acknowledgments

This research was sponsored by the National Science Council, Taiwan under Contract No. NSC96-2811-E-002-022.

References

[1] Lange F F 1989 *J. Am. Ceram. Soc.* **72** 3
[2] Chappat M 1994 *Colloids Surf.* A **91** 57
[3] Barnes H A 1994 *Colloids Surf.* A **91** 89
[4] Pons R, Solans C and Tadros Th F 1995 *Langmuir* **11** 1966
[5] An L, Riedel R, Konetschny C, Kleebe H J and Raj R 1998 *J. Am. Ceram. Soc.* **81** 1349
[6] Manga M, Castro J, Cashman K V and Loewenberg M 1998 *J. Volcanol. Geotherm. Res.* **87** 15
[7] Chu T M G and Halloran J W 2000 *J. Am. Ceram. Soc.* **83** 2189
[8] Buffo R A and Reineccius G A 2002 *J. Food Eng.* **51** 267
[9] Dan D and Jing G 2006 *J. Pet. Sci. Eng.* **53** 113
[10] Einstein A 1906 *Ann. Phys.* **19** 289
[11] Vand V 1948 *J. Phys. Colloid Chem.* **52** 277
[12] Peterson J M and Fixman M 1963 *J. Chem. Phys.* **39** 2516
[13] Batchelor G K and Green J T 1972 *J. Fluid Mech.* **56** 401
[14] Bedeaux D, Kapral R and Mazur P 1977 *Physica* A **88** 88
[15] Freed K F and Muthukumar M 1982 *J. Chem. Phys.* **76** 6186
[16] Cichocki B and Felderhof B U 1990 *J. Chem. Phys.* **93** 4427
[17] Thomas C U and Muthukumar M 1991 *J. Chem. Phys.* **94** 5180
[18] Beenakker C W J 1984 *Physica* A **128** 48
[19] Hsueh C H 2005 *J. Am. Ceram. Soc.* **88** 1046
[20] Taylor G I 1932 *Proc. R. Soc. Lond, Ser.* A **138** 41
[21] Bruggeman D A G 1935 *Ann. Phys.* **24** 636
[22] Roscoe R 1952 *Brit. J. Appl. Phys.* **3** 267
[23] Phan-Thien N and Pham D C 1997 *J. Non-Newton. Fluid Mech.* **72** 305
[24] Eshelby J D 1957 *Proc. R. Soc. London* A **241** 376
[25] Mori T and Tanaka K K 1973 *Acta Metall.* **21** 571
[26] Hsueh C H 1989 *J. Am. Ceram. Soc.* **72** 344
[27] Mase G E 1970 *Schaum's Outline Series: Theory and Problems of Continuum Mechanics* (New York: McGraw-Hill)
[28] Arfken G B 1970 *Mathematical Methods for Physicists* (New York: Academic)
[29] Christensen R M 1990 *J. Mech. Phys. Solids* **38** 397
[30] Hashin Z and Shtrikman S 1963 *J. Mech. Phys. Solids* **11** 127
[31] Lejeune A M, Bottinga Y, Trull T W and Richet P 1999 *Earth Planet. Sci. Lett.* **166** 71
[32] Stein D J and Spera F J 2002 *J. Volcanol. Geotherm. Res.* **113** 243
[33] Hsueh C H, Evans A G, Cannon R M and Brook R J 1986 *Acta Metall.* **34** 927
[34] Bedeaux D 1983 *Physica* A **121** 345
[35] Krieger I M and Dougherty T J 1959 *Trans. Soc. Rheol.* **3** 137
[36] Manga M and Loewenberg M 2001 *J. Volcanol. Geotherm. Res.* **105** 19